

Ly α and UV emission from high-redshift GRB hosts: To what extent do GRBs trace star formation?*

P. Jakobsson,^{1,2†} G. Björnsson,² J. P. U. Fynbo,¹ G. Jóhannesson,² J. Hjorth,¹
B. Thomsen,³ P. Møller,⁴ D. Watson,¹ B. L. Jensen,¹ G. Östlin,⁵ J. Gorosabel^{6,7}
and E. H. Gudmundsson²

¹Niels Bohr Institute, University of Copenhagen, Juliane Maries Vej 30, DK-2100 Copenhagen, Denmark

²Science Institute, University of Iceland, Dunhaga 3, 107 Reykjavík, Iceland

³Department of Physics and Astronomy, University of Aarhus, Ny Munkegade, DK-8000 Århus C, Denmark

⁴European Southern Observatory, Karl-Schwarzschild-Straße 2, 85748, Garching bei München, Germany

⁵Stockholm Observatory, SE-106 91 Stockholm, Sweden

⁶IAA-CSIC, P.O. Box 03004, E-18080 Granada, Spain

⁷Space Telescope Science Institute, 3700 San Martin Drive, Baltimore, MD 21218, USA

Accepted 2005 May. Received 2005 May 26; in original form 2005 April 11

ABSTRACT

We report the result of a search for Ly α emission from the host galaxies of the gamma-ray bursts (GRBs) 030226 ($z = 1.986$), 021004 ($z = 2.335$) and 020124 ($z = 3.198$). We find that the host galaxy of GRB 021004 is an extended (around 8 kpc) strong Ly α emitter with a restframe equivalent width (EW) of 68^{+12}_{-11} Å, and a star-formation rate of $10.6 \pm 2.0 M_{\odot} \text{ yr}^{-1}$. We do not detect the hosts of GRB 030226 and GRB 020124, but the upper limits on their Ly α fluxes do not rule out large restframe EWs. In the fields of GRB 021004 and GRB 030226 we find seven and five other galaxies, respectively, with excess emission in the narrow-band filter. These galaxies are candidate Ly α emitting galaxies in the environment of the host galaxies. We have also compiled a list of all $z \gtrsim 2$ GRB hosts, and demonstrate that a scenario where they trace star formation in an unbiased way is compatible with current observational constraints. Fitting the $z = 3$ luminosity function (LF) under this assumption, results in a characteristic luminosity of $R^* = 24.6$ and a faint end slope of $\alpha = -1.55$, consistent with the LF measured for Lyman-break galaxies.

Key words: dust, extinction – galaxies: evolution – galaxies: formation – galaxies: high-redshift – gamma-rays: bursts.

1 INTRODUCTION

Ly α photons face a large probability of being absorbed by dust particles due to resonant scattering. Therefore, Ly α emitting galaxies are often considered to contain little or no dust and to have low metallicity (Charlot & Fall 1993). However, a number of local metal-poor galaxies with active star formation show little signs of Ly α emission (e.g.

Mas-Hesse et al. 2003; Hayes et al. 2005). In addition, the luminous dusty SCUBA galaxies often display Ly α in emission (Chapman et al. 2003). This indicates that dust and metallicity are not the only factors affecting the escape of Ly α photons; kinematical and geometrical properties of the interstellar medium may also play a major part (e.g. Neufeld 1991; Giavalisco et al. 1996). Assuming, however, the validity of the Charlot & Fall (1993) relation between metallicity and Ly α emission (see their fig. 8), implies that Ly α imaging is a probe of the star-formation rate (SFR), dust content and metallicity

It is now firmly established that long-duration gamma-ray bursts (GRBs) are associated with star formation (e.g. Christensen et al. 2004) and, at least some, with core collapse supernovae (e.g. Hjorth et al. 2003b; Stanek et al. 2003; Malesani et al. 2004; Thomsen et al. 2004). Ly α observations of GRB host galaxies provide information about

* Based on observations made with the Nordic Optical Telescope, operated on the island of La Palma jointly by Denmark, Finland, Iceland, Norway, and Sweden, in the Spanish Observatorio del Roque de los Muchachos of the Instituto de Astrofísica de Canarias. Based on observations collected at the European Southern Observatory Very Large Telescope under programme 071.B-0199(A).

† E-mail: pallja@astro.ku.dk

their SFR, dust content and metallicity, knowledge which is crucial for our understanding of GRBs, their progenitors and environment. Furthermore, metallicity is an important parameter in some progenitor models. A high metallicity produces a strong stellar wind, which in turn leads to mass loss and loss of angular momentum. In the collapsar model these circumstances make it extremely problematic to generate a GRB (MacFadyen & Woosley 1999; see also Petrovic et al. 2005); a preference for GRB hosts to be metal-poor is therefore an unambiguous prediction of the collapsar model (assuming that the progenitor and host follow the same metallicity distribution). Alternative progenitor models exist where there is no such low metallicity preference (e.g. Ouyed et al. 2005; Fryer & Heger 2005).

There is growing evidence that the majority of GRB host galaxies, at least at high- z , are Ly α emitters (Fynbo et al. 2003a). If we define a Ly α emitter as having a Ly α restframe equivalent width (EW) larger than 10 Å, all of the five possible detections are confirmed Ly α emitters: GRB 971214 at $z = 3.42$ (Kulkarni et al. 1998; Ahn 2000), GRB 000926 at $z = 2.04$ (Fynbo et al. 2002, hereafter F02), GRB 011211 at $z = 2.14$ (Fynbo et al. 2003a), GRB 021004 at $z = 2.34$ (Møller et al. 2002) and GRB 030323 at $z = 3.37$ (Vreeswijk et al. 2004). For the latter two bursts, the Ly α emission line was detected superimposed on the afterglow spectrum. In addition, there is an indication of a Ly α emission line in the centre of the Ly α absorption trough in the GRB 030429 ($z = 2.66$) afterglow spectrum, although at a low significance level (Jakobsson et al. 2004a). As the GRB 030429 host is faint ($R > 26.3$) it would imply a relatively high EW.

In this paper we present a study of the host galaxies and environments of GRB 021004 ($z = 2.335$), GRB 030226 ($z = 1.986$) and GRB 020124 ($z = 3.198$). The properties of GRB 021004 and its afterglow have been discussed in, e.g. Holland et al. (2003), Nakar et al. (2003), Matheson et al. (2003) and Bersier et al. (2003). Its host is, like most previously studied GRB hosts, a very blue starburst galaxy ($R \approx 24.5$) with no evidence for dust (Fynbo et al. 2005c), whereas in the case of GRB 030226 there is no evidence for an underlying host galaxy ($R > 26.2$; Klose et al. 2004). GRB 020124 occurred in a very faint ($R > 29.5$; Berger et al. 2002) gas-rich galaxy with evidence for GRB surroundings with low dust content (Hjorth et al. 2003a).

We adopt a cosmology where the Hubble constant is $H_0 = 70 \text{ km s}^{-1} \text{ Mpc}^{-1}$, $\Omega_m = 0.3$ and $\Omega_\Lambda = 0.7$. For these parameters, a redshift of (1.986, 2.335, 3.198) corresponds to a luminosity distance of (15.41, 18.77, 27.45) Gpc and a distance modulus of (45.9, 46.4, 47.2). One arcsecond is equivalent to (8.38, 8.18, 7.55) proper kiloparsecs, and the lookback time is (10.2, 10.7, 11.5) Gyr.

2 OBSERVATIONS & DATA REDUCTION

The observations were carried out during one night (two nights were lost due to bad weather) in October 2003 (GRB 021004) and four nights in March 2004 (GRB 030226) at the 2.56-m Nordic Optical Telescope (NOT) on La Palma, using the MOSaic CAmera (MOSCA). The MOSCA detector consists of four 2048×2048 CCDs with a pixel scale of $0''.217$ (2×2 binning). The field of GRB 021004

Table 1. Total exposure time (in hours) and seeing in the combined image for each filter. GRB 021004 was observed in B , while GRB 030226 was observed in U . Note that when comparing the exposure times, GRB 020124 was observed with an 8-m telescope.

GRB	R		B/U		Narrow-band	
	Exp.	Seeing	Exp.	Seeing	Exp.	Seeing
021004	0.7	$1''.0$	1.4	$0''.8$	5.0	$0''.9$
030226	2.1	$1''.5$	7.2	$1''.3$	20.0	$1''.3$
020124	—	—	—	—	5.7	$0''.8$

(GRB 030226) was imaged in three filters: the standard B (U) and R filters and a special narrow-band filter manufactured by Omega Optical. The narrow-band filters were tuned to Ly α at $z = 2.331$ ($\lambda_{\text{cen}} = 4050 \text{ \AA}$) and $z = 1.986$ ($\lambda_{\text{cen}} = 3630 \text{ \AA}$) and had a width of $\Delta\lambda = 60 \text{ \AA}$ (corresponding to a redshift width of $\Delta z = 0.049$ for Ly α). GRB 020124 was observed during several nights in March and April 2003 with the Very Large Telescope in Chile, using the FOCal Reducer and low dispersion Spectrograph (FORS1). The FORS1 detector consists of a single 2048×2048 CCD with a pixel scale of $0''.20$. As this was a Category B service mode programme, our observations were not completed, resulting in a total of only 5.7 h of narrow-band imaging¹. An existing narrow-band filter, OIII/6000+52 ($\lambda_{\text{cen}} = 5105 \text{ \AA}$) with a width of $\Delta\lambda = 61 \text{ \AA}$, was used. For all three fields, the observations were carried out more than a year from the onset of the burst. An optical afterglow (OA) contribution is therefore negligible.

The individual exposures were bias-subtracted and flat-field corrected using standard techniques. The individual reduced images were combined using a σ -clipping routine optimised for faint sources (see details in Møller & Warren 1993). The total integration times along with the seeing in the combined images are given in Table 1. Narrow-band flux calibration was performed using observations of the spectrophotometric standard stars BD+28, GD71 and Hz44. The broadband images were calibrated using the Henden (2002, 2003) secondary standards. The transformations given in Fukugita et al. (1995) were finally used to bring the observations onto the AB-system. Conditions were not photometric when the NOT data were obtained, resulting in the narrow-band zeropoints being affected by clouds. Hence, they had to be adjusted as detailed in Sect. 3.1. This effect has not been taken into account in the uncertainties quoted in the paper.

3 RESULTS

We have used the same methods for photometry and selection of Ly α emitting galaxy candidates as those described in F02. In the following we will use the acronym LEGOs for Ly α Emitting Galaxy-building Objects, introduced by Møller & Fynbo (2001).

¹ A total of 18 hr were granted to the programme (to observe the GRB 020124 host).

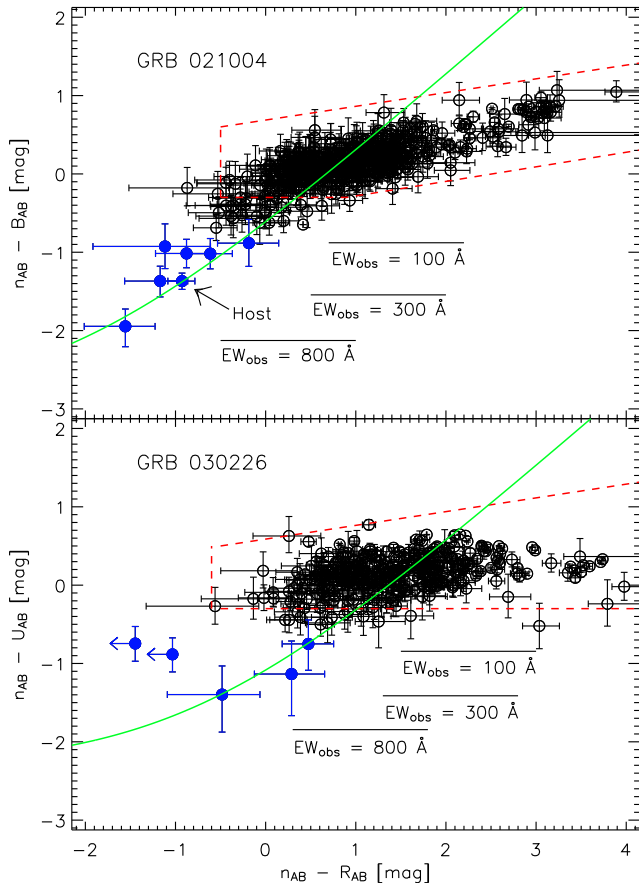


Figure 1. Colour-colour diagram for all objects detected at $S/N > 5$ in the narrow-band image, in the fields of GRB 021004 (top) and GRB 030226 (bottom). The dashed box encloses an area where all the model galaxy spectra are located (see main text for details). As expected, most objects have colours consistent with being in this box. However, a number of objects, including the GRB 021004 host, are located in the lower left part of the diagrams. The filled circles indicate LEGO candidates. The solid curve corresponds to objects having the same broadband colours, but various amounts of absorption (upper part) or emission (lower part) in the narrow-band filter.

3.1 GRB 021004

In the upper part of Fig. 1, the $n_{AB}-B_{AB}$ versus $n_{AB}-R_{AB}$ colour-colour diagram is plotted for the detected objects in the GRB 021004 field. The colours have not been corrected for Galactic extinction; such a correction would be negligible for $n_{AB}-B_{AB}$ and only shift objects slightly to the left (thus not affecting the number of LEGOs detected). In order to constrain where objects with no special features in the narrow-band filter fall in the diagram, we have calculated colours based on the synthetic galaxy spectra without Ly α emission provided by Bruzual & Charlot (1993). We have used models with ages ranging from a few Myr to 15 Gyr, with $0 < z < 3$. The box in Fig. 1 indicates the area where these model galaxies are located.

As mentioned above the narrow-band zeropoints for the NOT data were affected by cirrus. They were adjusted by requiring that the colours of objects detected at fairly high signal-to-noise ratio (S/N) would fall on the locus of the model galaxies. The resulting change in the narrow-band

Table 2. Photometric properties of the seven LEGO candidates in the field of GRB 021004. The GRB 021004 host galaxy is denoted by S1004.5.

Object	R_{AB} [mag]	B_{AB} [mag]	$f(\text{Ly}\alpha)$ [10^{-17} erg $\text{s}^{-1} \text{cm}^{-2}$]	SFR(Ly α) [$M_{\odot} \text{yr}^{-1}$]
S1004_1	$23.83^{+0.22}_{-0.19}$	$24.41^{+0.16}_{-0.14}$	11.8 ± 3.6	5.0 ± 1.5
S1004_2	$24.22^{+0.24}_{-0.19}$	$25.23^{+0.25}_{-0.20}$	3.2 ± 1.7	1.4 ± 0.7
S1004_3	$24.98^{+0.52}_{-0.35}$	$25.41^{+0.29}_{-0.23}$	10.2 ± 3.2	4.3 ± 1.4
S1004_4	$25.49^{+1.23}_{-0.56}$	$25.00^{+0.21}_{-0.18}$	7.2 ± 2.4	3.1 ± 1.0
S1004_5	$24.18^{+0.33}_{-0.25}$	$24.43^{+0.16}_{-0.14}$	25.1 ± 4.8	10.6 ± 2.0
S1004_6	$24.92^{+0.48}_{-0.33}$	$25.43^{+0.30}_{-0.23}$	11.3 ± 4.0	4.8 ± 1.7
S1004_7	$24.22^{+0.18}_{-0.15}$	$25.42^{+0.23}_{-0.19}$	3.2 ± 1.7	1.4 ± 0.7

Table 3. Photometric properties of the five LEGO candidates in the field of GRB 030226.

Object	R_{AB} [mag]	U_{AB} [mag]	$f(\text{Ly}\alpha)$ [10^{-17} erg $\text{s}^{-1} \text{cm}^{-2}$]	SFR(Ly α) [$M_{\odot} \text{yr}^{-1}$]
S0226_1	$24.27^{+0.15}_{-0.13}$	$24.91^{+0.10}_{-0.09}$	2.3 ± 1.2	0.7 ± 0.3
S0226_2	$24.62^{+0.17}_{-0.15}$	$25.32^{+0.11}_{-0.10}$	3.5 ± 1.8	1.0 ± 0.5
S0226_3	$24.81^{+0.21}_{-0.18}$	$25.97^{+0.21}_{-0.18}$	2.7 ± 1.6	0.8 ± 0.5
S0226_4	>24.9	$25.45^{+0.27}_{-0.22}$	4.9 ± 1.9	1.4 ± 0.5
S0226_5	>24.9	$25.16^{+0.11}_{-0.10}$	2.4 ± 1.0	0.7 ± 0.3

zeropoint was approximately 25%, with an uncertainty of approximately 5%.

LEGOs will fall in the lower left corner of the diagram, due to excess emission in the narrow-band filter. We select as LEGO candidates objects detected at more than 5σ in the narrow-band image and with a colour $n_{AB}-B_{AB} < -0.7$. This corresponds to an observed EW of about 67 \AA , or 20 \AA in the restframe for Ly α at $z = 2.335$. We find seven candidates in the field, including the host galaxy. Images of these LEGOs are shown in the left part of Fig. 2 and their photometric properties based on the total magnitudes (`mag_auto`) from SExtractor (Bertin & Arnouts 1996) are given in Table 2. The Ly α line flux is calculated by dividing the flux in the narrow-band filter with $1 + \Delta\lambda/\text{EW}_{\text{obs}}$. We also derive the SFR for the LEGOs, assuming that a Ly α luminosity of $10^{42} \text{ erg s}^{-1}$ corresponds to a SFR of $1 M_{\odot} \text{ yr}^{-1}$ (Kennicutt 1998; Cowie & Hu 1998). These SFRs should be considered as lower limits, since the estimates might be affected by extinction.

The host galaxy of GRB 021004 is detected in all bands and is a Ly α emitter with a restframe EW of $68^{+12}_{-11} \text{ \AA}$. Deep HST/ACS images of the host have been reported by Fynbo et al. (2005c). These images show that the host is dominated by a single component with the *fwhm* extending over $0''.12$ or roughly 1 kpc at $z = 2.335$. In Fig. 3 the contours of the Ly α emission are overplotted on an HST/ACS/WFC image, obtained 239 days after the burst. The Ly α weighted centroid is located very close to (and is consistent with) the centre of the galaxy, where the GRB originated. The extent of the Ly α emission is much larger than that of the continuum emission (about $1''.0$ after correcting for the seeing). A similar difference between contin-

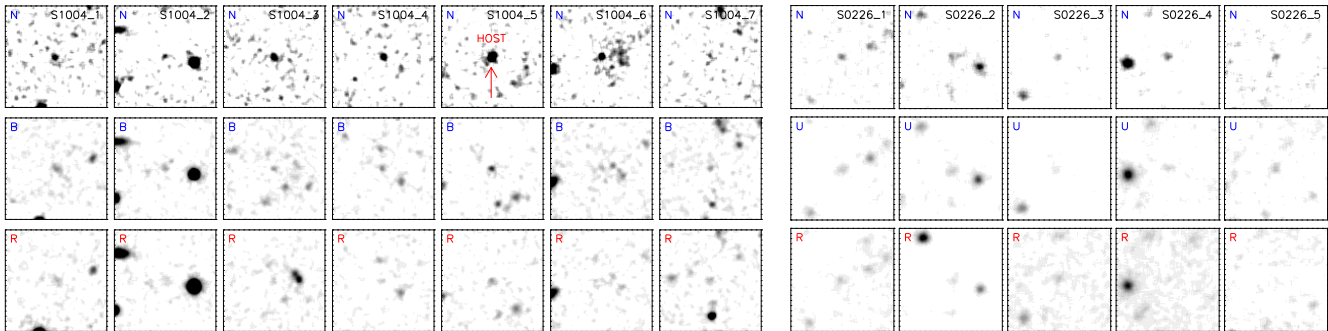


Figure 2. A $10'' \times 10''$ section around each of the LEGOs in the field of view of GRB 021004 (left) and GRB 030226 (right). For each candidate we show a sub-image from all three filters: narrow-band (top row), B -band or U -band (middle row) and R -band (bottom row). North is up and east is to the left. The GRB 021004 host is named S1004_5.

uum and $\text{Ly}\alpha$ emitting regions is seen both for other high- z $\text{Ly}\alpha$ emitters (e.g. Fynbo et al. 2003b) and for local starburst galaxies (Hayes et al. 2005).

3.2 GRB 030226

The host galaxy of GRB 030226 is not detected in any of the bands. We can set an upper limit (5σ) of $n_{\text{AB}} \approx 25.8$, corresponding to an observed emission line flux of $2.4 \times 10^{-17} \text{ erg s}^{-1} \text{ cm}^{-2}$. We calculate the broadband limiting magnitudes (2σ) in a circular aperture with a radius equal to the seeing, resulting in $R_{\text{AB}} \approx 24.9$ and $U_{\text{AB}} \approx 26.2$. In Fig. 4 we show a $10'' \times 10''$ region containing the position of the afterglow from a weighted sum of the combined $\text{Ly}\alpha$ and U -band images. The weight is calculated as the variance of the background after scaling to the same flux level. We detect no significant emission from the host above an estimated 2σ limit of $U_{\text{AB}} \approx 26.5$.

In the lower part of Fig. 1, the $n_{\text{AB}}-U_{\text{AB}}$ versus $n_{\text{AB}}-R_{\text{AB}}$ colour-colour diagram is plotted for the detected objects in the GRB 030226 field. We have followed a similar procedure as in Sect. 3.1 to select the LEGOs, resulting in the detection of five candidates. Here the colour criteria is $n_{\text{AB}}-U_{\text{AB}} < -0.6$, corresponding to an observed EW of about 60 \AA , or 20 \AA in the restframe for $\text{Ly}\alpha$ at $z = 1.986$. The LEGO images are shown in the right part of Fig. 2 and their photometric properties are given in Table 3.

3.3 GRB 020124

Lacking broadband observations for the GRB 020124 field, we are unable to identify LEGO candidates. The host galaxy is not detected above a limit of $1.5 \times 10^{-17} \text{ erg s}^{-1} \text{ cm}^{-2}$ (5σ) in the narrow-band image. Since the host is very faint (Berger et al. 2002), this non-detection does not exclude a large $\text{Ly}\alpha$ EW (see below). In Fig. 4 we show a $10'' \times 10''$ region centred on the position of the afterglow.

3.4 Foreground Interlopers

Low-redshift galaxies with other emission lines in the narrow-band filter can mimic the high-redshift $\text{Ly}\alpha$ candidates we are aiming at (e.g. Stern et al. 2000). For the GRB 021004 host, the redshift is known from spectroscopy (Møller et al. 2002). For the remaining LEGO candidates,

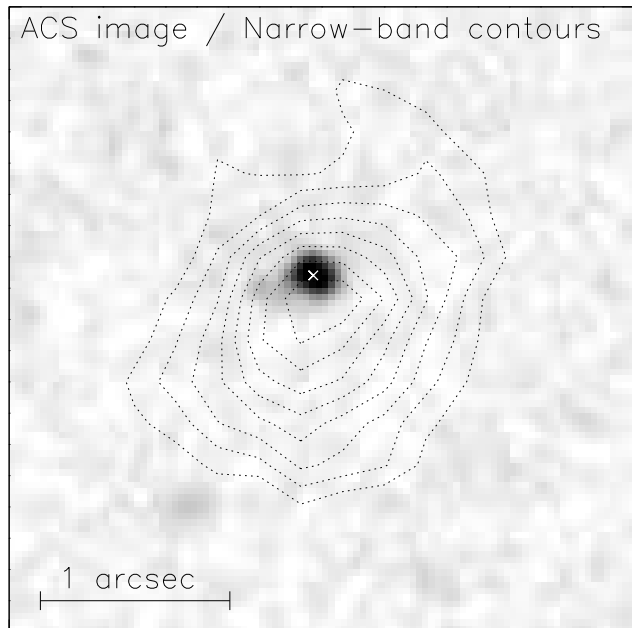


Figure 3. A $3'' \times 3''$ section of an HST/ACS/WFC image centered on the host galaxy of GRB 021004. It was obtained on 2003 May 31, approximately 239 days after the burst. The contours show the $\text{Ly}\alpha$ emission based on the narrow-band observations (with a seeing of $0''.9$). The GRB (position marked with a cross) went off near the centre of the galaxy. North is up and east is to the left.

other emission line sources than $\text{Ly}\alpha$ are possible. We can exclude foreground galaxies with $[\text{OII}] \lambda 3727$ in the GRB 021004 narrow-band filter, since such objects would have to be at a very low redshift ($z = 0.09$) and hence be much brighter than our candidates. Other possible explanations are CIV at $z = 1.34$ (GRB 030226) and $z = 1.61$ (GRB 021004), and MgII at $z = 0.30$ (GRB 030226) and $z = 0.45$ (GRB 021004). The presence of strong CIV and MgII emission requires an underlying active galactic nucleus (AGN). We have carried out a similar calculation as in F02 to show that the probability, that the expected number of AGNs in our field of view fall in the aforementioned small volumes, is of the order of 1%. Therefore, significant MgII and CIV contamination due to AGNs is not expected.

Table 4. A list of all GRBs with $z > 1.9$ known to date (May 2005). The detection method indicates how Ly α in emission was detected. The host magnitudes are given in the Cousins/Johnson photometric system and have been corrected for Galactic extinction (Schlegel et al. 1998). The restframe wavelength is obtained by dividing the observed wavelength by $(1+z)$. References are given in order for: redshift, Ly α EW_{rest} and host magnitude. (1) Kulkarni et al. (1998); (2) S.-H. Ahn (private communication); (3) Odewahn et al. (1998); (4) Andersen et al. (2000); (5) This work; (6) Jensen et al. (2001); (7) F02; (8) Fruchter & Vreeswijk (2001); (9) Castro et al. (2003); (10) Fruchter et al. (2001); (11) Fynbo et al. (2003a); (12) Jakobsson et al. (2003); (13) Hjorth et al. (2003a); (14) Berger et al. (2002); (15) Møller et al. (2002); (16) Fynbo et al. (2005c); (17) Klose et al. (2004); (18) Vreeswijk et al. (2004); (19) Jakobsson et al. (2004a); (20) Kelson & Berger (2005); (21) Gorosabel et al. (2005); (22) Fynbo et al. (2005a); (23) Fynbo et al. (2005b); (24) Prochaska et al. (2005); (25) Cenko et al. (2005); (26) Berger et al. (2005); (27) Chapman et al. (2005).

GRB	z	Ly α EW _{rest} [Å]	Detection method	Host mag	Restframe wavelength [Å]	Host mag ($z = 3$)	References
971214	3.42	~ 14	Ly α line in host spectrum	$R = 26.5$	1490	26.4	(1) (2) (3)
000131	4.50	—		$I = 26.4$	1465	26.2	(4) (5)
000301C	2.04	$\lesssim 150$		$R = 27.9$	2165	28.1	(6) (7) (8)
000926	2.04	71^{+20}_{-15}	Narrow-band Ly α imaging	$U = 23.9$	1200	24.1	(9) (7) (7)
011211	2.14	21^{+11}_{-8}	Narrow-band Ly α imaging	$R = 25.0$	2095	25.2	(10) (11) (12)
020124	3.20	—		$R > 29.4$	1565	> 29.4	(13) (14)
021004	2.34	68^{+12}_{-11}	Narrow-band Ly α imaging	$B = 24.3$	1330	24.4	(15) (5) (16)
030226	1.99	—		$U > 25.7$	1220	> 25.9	(17) (5)
030323	3.37	~ 145	Ly α line in OA spectrum	$V = 27.9$	1260	27.8	(18) (18) (18)
030429	2.66	—		$R > 26.1$	1800	> 26.2	(19) (19)
050315	1.95	—		$R = 23.8$	2230	24.0	(20) (21)
050319	3.24	—		$R > 25.0$	1550	> 25.0	(22) (5)
050401	2.90	—		$R > 25.3$	1685	> 25.3	(23) (5)
050502A	3.79	—		$R > 23.5$	1305	> 23.4	(24) (25)
050505	4.27	—		$R > 21.5$	1250	> 21.3	(26) (27)

4 DISCUSSION

4.1 LEGOs

We compare the properties of the LEGO candidates in the fields of GRB 021004 and GRB 030226 to properties of $z \approx 2$ galaxies found in other surveys. The survey parameters (including flux limits) of Kurk et al. (2000) and Pentericci et al. (2000), who have detected and spectroscopically confirmed 15 LEGOs (including the radio galaxy) in the field around PKS 1138–262 at $z = 2.156$, are similar to ours. Their inferred number of LEGOs per arcmin² per unit redshift is 7.8 ± 2.0 . The corresponding number for the fields of GRB 000301C and GRB 000926 (F02) is 8.3 ± 2.0 . In addition, Fynbo et al. (2003a) find ~ 4.5 LEGOs per arcmin² per unit redshift in the field of GRB 011211.

We observe 12 LEGO candidates in two ~ 50 arcmin² fields with a filter spanning $\Delta z = 0.049$. This corresponds to ~ 2.5 LEGOs per arcmin² per unit redshift. We note that the MOSCA field of view is around 60 arcmin², but the combined effect of the relatively large chip gaps ($\sim 8''$) and image dithering resulted in a loss of approximately 10 arcmin². The LEGO mean density for the five GRB fields observed thus far is about 5.6, consistent with that found around PKS 1138–262. Unfortunately, there are currently no similar (in redshift and depth) surveys for Ly α emitters in blank fields. Thus, the number of LEGOs representing the mean density at $z \approx 2$ is uncertain. But there is some evidence that GRB host galaxies do not reside in high galaxy density environments (Bornancini et al. 2004; Foley et al. in preparation).

4.2 Ly α Emission from the GRB Hosts

This study confirms what is already known about GRB 021004, namely that its host is a strong Ly α emitter with a restframe EW of 68^{+12}_{-11} Å, consistent with the value of 69 ± 14 Å estimated by Fynbo et al. (2005c) from a ground-based spectrum. The lack of Ly α emission from the hosts of GRB 030226 and GRB 020124 in our deep narrow-band images does not rule out large restframe EWs. Assuming a GRB 020124 host magnitude of $R_{AB} \approx 29.5$ (consistent with the deep limit from Berger et al. 2002), a restframe Ly α EW of ~ 500 Å would have remained undetectable. The corresponding value for GRB 030226, assuming a host magnitude of $U_{AB} \approx 26.5$, is ~ 40 Å. Fainter host magnitudes would result in even higher restframe EW limits.

4.3 Are GRBs Biased Tracers of Star Formation?

All current evidence is consistent with the conjecture that the host galaxies of GRBs, at least at high redshifts ($z \gtrsim 2$), are Ly α emitters. An explanation could be an OA selection bias against dusty hosts (e.g. Tanvir et al. 2004, and references therein). However, the fraction of truly dark bursts is perhaps as small as 10% (e.g. Fynbo et al. 2001; Berger et al. 2002; Lamb et al. 2004; Jakobsson et al. 2004b, 2005). This suggests that GRB-selected galaxies should not be biased against very dusty systems.

A low metallicity preference for GRB progenitors, at least at high- z , is a possible interpretation of our results (Fynbo et al. 2003a). In this case GRBs could be *biased* tracers of star formation (e.g. Le Floch 2003). It is therefore of interest to consider whether our results are consistent with the hypothesis that GRBs are *unbiased* tracers of star

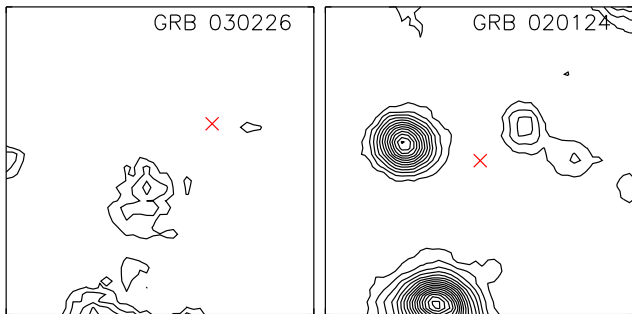


Figure 4. The location of GRB030226 (left) and GRB020124 (right) as imaged in the combined $\text{Ly}\alpha + U$ -band (left) and $\text{Ly}\alpha$ (right). The size of the images is $10'' \times 10''$. The position of the optical afterglows (OAs) is indicated with a cross. In both panels, the OA positional uncertainty is smaller than the extent of the cross. No significant emission at the burst positions is detected. North is up and east is to the left.

formation between approximately $2 \lesssim z \lesssim 4$, where the majority of known high- z GRBs are located, and where the peak of the star-formation activity is situated.

In order to test this hypothesis we have collected all high- z ($z \gtrsim 2$) GRB host galaxies reported in the literature, together with their redshifts, $\text{Ly}\alpha$ restframe EW if available, host magnitudes and host magnitudes redshifted to $z = 3$, assuming a flat F_ν spectrum (Table 4). Assuming that GRBs trace UV luminosity we fit the $z = 3$ magnitudes to the Schechter (1976) luminosity function (LF), including the upper limits as described in Appendix A. We find a characteristic magnitude of $24.6^{+0.6}_{-0.7}$ mag and a faint end slope of $\alpha = -1.55^{+0.24}_{-0.16}$ (the 1σ contour is shown in Fig. 5). We compare this to the R -band LF, corresponding to the restframe UV LF, for Lyman-break galaxies (LBGs) at $z = 3$. The LBG LF has a characteristic magnitude of 24.54 ± 0.14 mag and a faint end slope of $\alpha = -1.57 \pm 0.14$ (Adelberger & Steidel 2000). Hence, there is consistency between the properties of the GRB host and LBG LFs, implying that GRBs are consistent with tracing the UV luminosity. Only $\sim 33\%$ of the $R < 25.5$ LBGs are $\text{Ly}\alpha$ emitters with a restframe EW larger than 10 \AA (Shapley et al. 2003), but if this fraction is higher at fainter magnitudes this could be consistent with the high fraction of $\text{Ly}\alpha$ emitters among GRB hosts.

The next question is whether UV luminosity on average is proportional to the SFR. Locally, such a correlation has been established (Kennicutt 1998), but it is known that for some starburst galaxies, most of the UV emission is absorbed and re-radiated by dust (e.g. Chapman et al. 2003). However, Chary & Elbaz (2001) argue that the contribution to the total SFR density at $z = 3$ from dust-enshrouded ultra-luminous IR galaxies (ULIRGs) is most likely less than 30%. Therefore it is a good first approximation to assume that the UV luminosity, for the bulk of the star-forming galaxies, is proportional to the SFR at $z = 3$. In conclusion, the available data do not exclude GRBs as star-formation tracers, but additional observations are clearly required to settle the issue.

If the mass-metallicity relation for galaxies (Tremonti et al. 2004) was already in place at $z \gtrsim 2$ (Møller et al. 2004; Ledoux et al. 2005), a natural interpre-

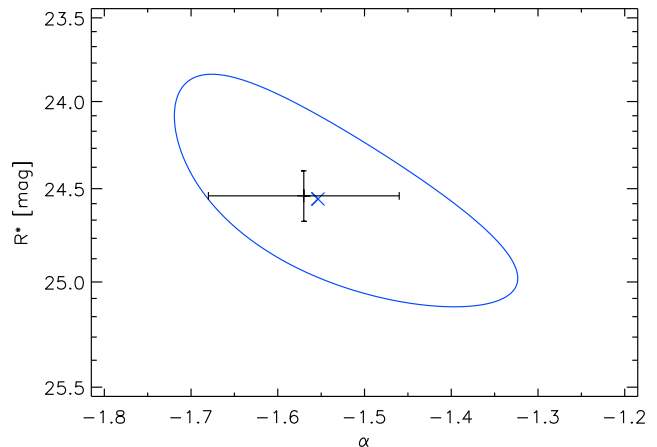


Figure 5. The 1σ confidence contour for the characteristic magnitude (R^*) and faint end slope (α) fitted under the assumption that GRBs trace star formation. The \times indicates the best fit. The point with errorbars marks the R^* and α range for LBGs (Adelberger & Steidel 2000).

tation of our $\text{Ly}\alpha$ results, is that GRB hosts predominantly are low-mass systems. It has been argued from redshift surveys that there is downsizing in galaxy formation, i.e. that the most massive galaxies form first and galaxy formation proceeds from larger to smaller mass scales (e.g. Juneau et al. 2005). This scenario, seemingly at odds with the hierarchical galaxy formation scenario, is not supported by the properties of high- z GRB host galaxies if they trace star formation: under this assumption, low-mass galaxies dominate the integrated star-formation density at high- z . The evidence from redshift surveys then only implies that star-formation activity in high-mass galaxies dies out faster than in low-mass galaxies, which seem to dominate at all redshifts.

5 SUMMARY

We have carried out a narrow-band $\text{Ly}\alpha$ imaging of three GRB host galaxies and their environments. The GRB021004 host ($z = 2.335$) is a strong $\text{Ly}\alpha$ emitter with a restframe EW of $68^{+12}_{-11} \text{ \AA}$. We do not detect the hosts of GRB030226 ($z = 1.986$) and GRB020124 ($z = 3.198$) in $\text{Ly}\alpha$; the 5σ upper limits are $2.4 \times 10^{-17} \text{ erg s}^{-1} \text{ cm}^{-2}$ and $1.5 \times 10^{-17} \text{ erg s}^{-1} \text{ cm}^{-2}$, respectively. We find a total of 12 LEGOs in the fields of GRB021004 and GRB030226.

We have also assembled a list of all GRB hosts at $z \gtrsim 2$ reported in the literature. The distribution of the host magnitudes is consistent with the LF of LBGs at $z = 3$. If the LBG restframe UV continuum is proportional to the SFR, this suggests that the hypothesis of GRBs as star-formation tracers is compatible with current observations. In addition, when applying the mass-metallicity relation (Tremonti et al. 2004), this would imply that low-mass galaxies dominate the integrated star-formation density at all epochs.

To clarify the situation we need a complete and unbiased sample of GRB host galaxies with measured redshifts in a well defined redshift range. This is necessary in order to exclude any remaining uncertainty on whether the current sample is biased against dusty host galaxies. The currently

operating *Swift* satellite (Gehrels et al. 2004) offers a unique possibility to secure such a sample. We also need an independent gauge of the SFR distribution function in the same well defined redshift range. One suitable redshift range is $z < 0.2$ where large redshift surveys, such as the Sloan Digital Sky Survey (SDSS, e.g. Abazajian et al. 2005) and the 2dF Galaxy Redshift Survey (2dFGRS, e.g. Colless et al. 2003), have provided an extensive census and where it is possible to firmly constrain the amount of obscured star formation. Another possible redshift range is $2 < z < 4$, where a plenitude of starburst selection techniques are available, e.g. LBGs, Ly α galaxies, sub-mm galaxies and distant red galaxies, and where the peak of the cosmic star-formation density appears to have been located.

ACKNOWLEDGMENTS

We thank Stephanie Courty for an intense and enlightening discussion on (specific) star formation, and the anonymous referee for a careful reading and useful corrections. P.J, GB and EHG gratefully acknowledge support from a special grant from the Icelandic Research Council. JPUF acknowledges support from the Carlsberg foundation. BLJ acknowledges support from the Instrument Centre for Danish Astrophysics (IDA) and the Nordic Optical Telescope (NOT). JG acknowledges the support of a Ramón y Cajal Fellowship from the Spanish Ministry of Education and Science. The research of JG is supported by the Spanish Ministry of Science and Education through programmes ESP2002-04124-C03-01 and AYA2004-01515. This work was supported by the Danish Natural Science Research Council. The authors acknowledge benefits from collaboration within the EU FP5 Research Training Network “Gamma-Ray Bursts: An Enigma and a Tool”. We are also grateful to the Nordic Optical Telescope Scientific Association (NOTSA) and the Science Institute, University of Iceland for financial support.

REFERENCES

- Adelberger K. L., Steidel C. C., 2000, *ApJ*, 544, 218
Ahn A.-H., 2000, *ApJ*, 530, L9
Andersen M. I. et al., 2000, *A&A*, 364, L54
Abazajian K. et al., 2005, *AJ*, 129, 1755
Berger E. et al., 2002, *ApJ*, 581, 981
Berger E. et al., 2005, *GCN Circ.* 3368
Bersier D. et al., 2003, *ApJ*, 584, L43
Bertin E., Arnouts S., 1996, *A&AS*, 117, 393
Bornancini C. G., Martínez H. J., Lambas D. G., Le Floch E., Mirabel I. F., Minniti D., 2004, *ApJ*, 614, 84
Bruzual A. G., Charlot S., 1993, *ApJ*, 405, 538
Castro S., Galama T. J., Harrison F. A., Holtzman J. A., Bloom J. S., Djorgovski S. G., Kulkarni S. R. et al., 2003, *ApJ*, 586, 128
Cenko S. B., Fox D. B., Cameron, P. B., 2005, *GCN Circ.* 3355
Chapman R. et al., 2005, *GCN Circ.* 3375
Chapman S. C., Blain A. W., Ivison R. J., Smail I. R., 2003, *Nat*, 422, 695
Charlot S., Fall S. M., 1993, *ApJ*, 415, 580
Chary R., Elbaz D., 2001, *ApJ*, 556, 562
Christensen L., Hjorth J., Gorosabel J., 2004, *A&A*, 425, 913
Colless M. et al., 2003 (*astro-ph/0306581*)
Cowie L. L., Hu E. M., 1998, *AJ*, 115, 1319
Fruchter A., Vreeswijk P., 2001, *GCN Circ.* 1063
Fruchter A., Vreeswijk P., Rhoads J., Burud I., 2001, *GCN Circ.* 1200
Fryer C. L., Heger A., 2005, *ApJ*, 623, 302
Fukugita M., Shimasaku K., Ichikawa T., 1995, *PASP*, 107, 945
Fynbo J. P. U. et al., 2001, *A&A*, 369, 373
Fynbo J. P. U. et al., 2002, *A&A*, 388, 425 (F02)
Fynbo J. P. U. et al., 2003a, *A&A*, 406, L63
Fynbo J. P. U. et al., 2003b, *A&A*, 407, 147
Fynbo J. P. U., Hjorth J., Jensen B. L., Jakobsson P., Møller P., Näränen J., 2005a, *GCN Circ.* 3136
Fynbo J. P. U. et al., 2005b, *GCN Circ.* 3176
Fynbo J. P. U. et al., 2005c, *ApJ*, submitted
Gehrels N. et al., 2004, *ApJ*, 611, 1005
Giavalisco M., Koratkar A., Calzetti D., 1996, *ApJ*, 466, 831
Gorosabel J. et al., 2005, *GCN Circ.* 3294
Hayes M., Östlin G., Mas-Hesse J. M., Kunth D., Leitherer C., Petrosian A., 2005, *A&A*, in press (*astro-ph/0503320*)
Henden A. A., 2002, *GCN Circ.* 1583
Henden A. A., 2003, *GCN Circ.* 1916
Hjorth J. et al., 2003a, *ApJ*, 597, 699
Hjorth J. et al., 2003b, *Nat*, 423, 847
Holland S. T. et al., 2003, *AJ*, 125, 2291
Jakobsson P. et al., 2003, *A&A*, 408, 941
Jakobsson P. et al., 2004a, *A&A*, 427, 785
Jakobsson P., Hjorth J., Fynbo J. P. U., Watson D., Pedersen K., Björnsson G., Gorosabel J., 2004b, *ApJ*, 617, L21
Jakobsson P. et al., 2005, *ApJ*, in press (*astro-ph/0505035*)
Jensen B. L. et al., 2001, *A&A*, 370, 909
Juneau S. et al., 2005, *ApJ*, 619, L135
Kelson D., Berger E., 2005, *GCN Circ.* 3101
Kennicutt R. C., 1998, *ARA&A*, 36, 189
Klose S. et al., 2004, *AJ*, 128, 1942
Kulkarni S. R. et al., 1998, *Nat*, 393, 35
Kurk J. D. et al., 2000, *A&A*, 358, L1
Lamb D. Q. et al., 2004, *NewAR*, 48, 423
Ledoux C., Møller P., Petijean P., Fynbo J. P. U., Srianand R., 2005, *A&A*, submitted
Le Floch E., 2003, *NewAR*, 48, 601
MacFadyen A. I., Woosley S. E., 1999, *ApJ*, 524, 262
Malesani D. et al., 2004, *ApJ*, 609, L5
Mas-Hesse J. M., Kunth D., Tenorio-Tagle G., Leitherer C., Terlevich R. J., Terlevich E., 2003, *ApJ*, 598, 858
Matheson T. et al., 2003, *ApJ*, 582, L5
Møller P., Fynbo J. P. U., 2001, *A&A*, 372, L57
Møller P., Warren S. J., 1993, *A&A*, 270, 43
Møller P. et al., 2002, *A&A*, 396, L21
Møller P., Fynbo J. P. U., Fall S. M., 2004, *A&A*, 422, L33
Nakar E., Piran T., Granot J., 2003, *NewA*, 8, 495
Neufeld D. A., 1991, *ApJ*, 370, L85
Odewahn S. C. et al., 1998, *ApJ*, 509, L5
Ouyed R., Rapp R., Vogt T., 2005, *ApJ*, submitted (*astro-ph/0503357*)
Pentericci L. et al., 2000, *A&A*, 361, L25

- Petrovic J., Langer N., Yoon S.-C., Heger A., 2005, A&A, in press (astro-ph/0504175)
 Prochaska J. X. et al., 2005, GCN Circ. 3332
 Schechter P., 1976, ApJ, 203, 297
 Schlegel D. J., Finkbeiner D. P., Davis M., 1998, ApJ, 500, 525
 Shapley A. E., Steidel C. C., Pettini M., Adelberger K. L., 2003, ApJ, 588, 65
 Stanek K. Z. et al., 2003, ApJ, 591, L17
 Stern D., Bunker A., Spinrad H., Dey A., 2000, ApJ, 537, 73
 Tanvir N. R. et al., 2004, MNRAS, 352, 1073
 Thomsen B. et al., 2004, A&A, 419, L21
 Tremonti C. A. et al., 2004, ApJ, 613, 898
 Vreeswijk P. M. et al., 2004, A&A, 419, 927

APPENDIX A: MAXIMUM LIKELIHOOD ANALYSIS

The Schechter luminosity function (LF) is given by:

$$\Phi(L)dL = \Phi^* \left(\frac{L}{L^*}\right)^\alpha \exp\left(-\frac{L}{L^*}\right) d\left(\frac{L}{L^*}\right),$$

where Φ^* is a number per unit volume and L^* is a characteristic luminosity (with an equivalent characteristic magnitude) at which the LF exhibits a rapid change in the slope in the $(\log \Phi, \log L)$ -plane. The dimensionless parameter α gives the slope of the LF in the $(\log \Phi, \log L)$ -plane when $L \ll L^*$.

If the probability of a GRB occurring in a galaxy is proportional to its UV luminosity, then the probability to find a GRB in a galaxy with UV luminosity L is proportional to $L \times \Phi(L)$. Normalising this probability density we find:

$$p(\alpha, L^*; L) = \frac{L^{\alpha+1} \exp(-L/L^*)}{(L^*)^{\alpha+2} \Gamma(\alpha+2)},$$

where Γ is the gamma-function. In the discussion we use the LBG restframe UV LF and compare with the sample of $z > 2$ GRB hosts.

Given the observed sample, we use the following likelihood function (LH) for L^* and α :

$$LH(\alpha, L^*) = \prod_{i=1}^N p(\alpha, L^*; L_i) \times \prod_{j=1}^M \int_0^{L_j} p(\alpha, L^*; L) dL,$$

where $N = 7$ is the number of GRB hosts with a detected luminosity (L_i) and $M = 6$ is the number of GRB hosts with a luminosity upper limit (L_j). The maximum likelihood corresponds to an observed R -band magnitude of 24.8 and a faint end slope of $\alpha = -1.53$ (Fig. 5). The 1σ error contour in the (R^*, α) -plane is found from the condition:

$$\log_e \frac{LH(\alpha, R^*)}{LH_{\max}} = -1/2.$$